科技部補助

大專學生研究計畫研究成果報告

計畫名稱：	背根神經節內注射表達Hes1的慢病毒載體抑制慢性壓迫性損傷中代謝型谷氨酸受體亞型5介導的機械性超敏反應

執行計畫學生：張晴

學生計畫編號：MOST 109-2813-C-040-043-B
研究期間：109年07月01日至110年02月28日止，計8個月
指導教授：曾拓榮

處理方式：本計畫可公開查詢

執行單位：中山醫學大學醫學系解剖學科

中華民國　110年03月26日

前言

Neuropathic pain resulting from peripheral nerve lesions or dysfunction remains one of the most challenging neurological diseases. The dorsal horn of the spinal cord is a main sensory relay center, where a pre-synaptic terminal excitation or inhibition modulates post-synaptic neuronal activity for establishing central sensitization. Nerve decompression is an essential therapeutic strategy for pain relief clinically; however, its potential mechanisms in the spinal cord remains poorly understood.

研究目的

To verify the metabotropic glutamate receptors (mGluRs)/protein kinase c (PKC) signaling in the spinal cord, which leads to chronic constriction injury (CCI)-induced mechanical hypersensitivity.

We propose experiments that nerve decompression in rats with CCI relieves mechanical hypersensitivity and extend these observations by

1) determining whether nerve decompression can affect the spinal plasticity of peptidergic and non-peptidergic nerve terminals,

2) determining whether mGluRs, including mGluR1 and mGluR5, are associated with CCI-induced mechanical hypersensitivity,

3) determining whether classical PKC, including PKCα, PKCβ and PKCr, are the downstream modulators of mGluRs,

4) determining whether the treatments of lentiviral vector expressing Hes1 in CCI rats by intra-DRG injections can attenuate CCI-induced mechanical hypersensitivity effectively.

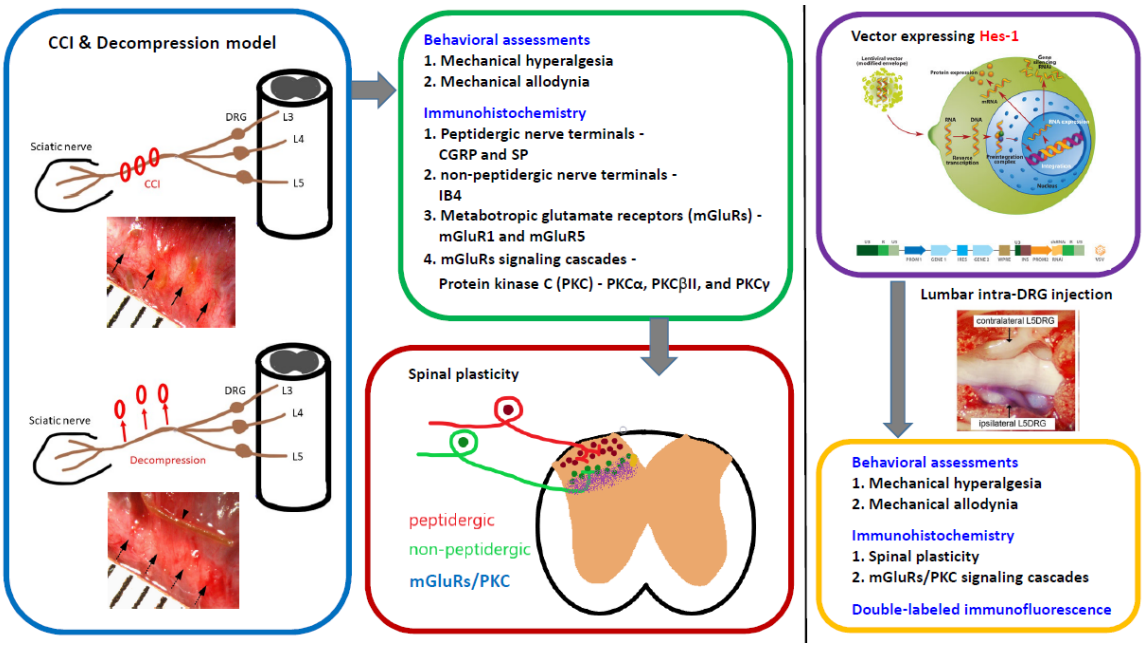

文獻探討

In clinical, nerve decompression is an essential surgical procedure resulting from the

compression or entrapment of various peripheral nerves (Padua et al., 2016; Thomson, 2017). Although its therapeutic efficacy is well-known, the underlying mechanism of its pain relief has remained poorly understood. Therefore, a most important neuropathic pain model, chronic constriction injury (CCI), has been established in rodents (Bennett and Xie, 1988). Importantly, we have found the nerve decompression shortens the durations of CCI-induced chronic pain, including thermal hyperalgesia and mechanical allodynia, for nearly 2 months (Tseng et al., 2007a; Tseng et al., 2008).

The dorsal horn of the spinal cord is a main sensory relay center, where a pre-synaptic terminal excitation or inhibition modulates post-synaptic neuronal activity for establishing central sensitization (Todd 2010; Ji et al. 2003; Woolf 2000). Our previous results indicate nerve decompression provides the opportunity for improving the spinal synaptic plasticity of mu- and delta-opioid receptors in the peptidergic nerve terminals (Tseng et al. 2008; Tseng et al. 2018). In addition, reversal of ERK activation in the dorsal horn neurons relieves CCI-induced chronic pain after nerve decompression (Tseng et al. 2007b).

The biological effects of glutamate in nociceptive mechanisms are mainly mediated by two major glutamate receptors: Ligand-gated ionotropic glutamate receptors (iGluRs) and G protein-coupled metabotropic glutamate receptors (mGluRs) (Crupi et al. 2019; Obara et al. 2013. L-glutamate is a principal excitatory neurotransmitter and known to participate in nociceptive signaling pathways by interacting with mGluRs (Obara et al. 2013). Earlier studies identify the group I mGluRs, including subtype 1 and 5 of mGluRs (mGluR1 and mGluR5), localized in primary afferents (Obara et al. 2013; Pereira and Goudet 2019). Additionally, the role of mGluR5 in inflammatory pain is supposed by coupling to inositol phosphate metabolism to modulate the neuronal excitability and synaptic transmission (Khan et al. 2019; Obara et al. 2013)

Regulated phosphorylation plays a well-documented role in modulating the biochemical, biophysical, and functional properties of the receptor (Wang et al. 2014). The common kinases include protein kinase A, protein kinase C (PKC), Calcium/calmodulin-dependent protein kinase II, Src/Fyn non-receptor tyrosine kinases, and cyclin dependent kinase-5 (Price and Inyang, 2015; Mochly-Rosen D et al. 2012). An increasing number of synapse-enriched protein kinases have been found to phosphorylate ionotropic glutamate receptors (iGluRs), including AMPA receptor and NMDA receptor (Wang et al. 2014; Mochly-Rosen D et al. 2012). Thus, it will be hot topics and could contribute to the development of novel pharmacotherapies, by targeting the defined phosphorylation process, for suppressing mGluRs-related disorders.

研究方法

Animals

Adult male Sprague-Dawley rats weighing 250–300 g used in these experiments are placed in a temperature- and humidity-controlled room with a 12 h light/dark cycle. All the procedures are conducted in accordance with the ethical guidelines set up by the International Association for the Study of Pain (IASP) on the use of laboratory animals in the experimental research and the protocol is approved by the Animal Committee of Chung Shan Medical University College of Medicine, Taichung, Taiwan (IASP Committee, 1980; Zimmermann, 1983).

Surgery

CCI is performed in rats following the established surgical procedures (Bennett and Xie, 1988). To examine the effect of nerve decompression on chronic pain, rats are randomly assigned to either CCI or Decompression as previously described (Tseng et al., 2007a). Before nerve decompression, all four ligatures are visible although reactive fibrosis became prominent at post-operative week (POW) 4. Under dissecting microscope (Olympus, Venter Valley, Pennsylvania, USA), ligatures could be untied without destroying the surrounding tissues, which is defined as Decompression. And sham-operated rats are investigated.

Behavioral assessments

1. Thermal hyperalgesia

Thermal hyperalgesia is evaluated with a Hargreaves-type analgesiometer (Ugo Basile, Comerio-Varese, Italy).

2. Mechanical allodynia

Mechanosensitivity is determined by measuring the withdrawal thresholds with a series of calibrated Von Frey filaments (Senselab aesthesiometer, Somedic Sales AB, Stockholm) according to an up-and-down method.

Immunohistochemistry

At the end of all experiments, the rats are deeply anesthetized using pentobarbital (100 mg/kg, i.p.) and sacrificed by intracardiac perfusion of 4% paraformaldehyde in 0.1 M phosphate buffer (PB) at pH 7.4. After perfusion, the spinal cords are removed and further immersed in fixative for additional 6 h before shifted to 0.1 M PB for storage. Prior to sectioning, samples are rinsing thoroughly, cryoprotected with 30% sucrose in 0.1 M PB overnight **;** then cut at a plane perpendicular to the epidermis in a thickness of 50 μm per

section with a sliding microtome (HM440E; Microm, Walldorf), labeled sequentially, and stored at -20℃. The sections for immunohistochemistry are treated with 0.5% Triton X-100 in 0.5 M Tris buffer (Tris) at pH 7.6 for 30 min and processed for immunostaining. Briefly, the sections are quenched with 1% H_2O_2 in methanol, blocked with 5% normal goat serum in 0.5% nonfat dry milk/Tris, then incubated with primary antiserum including (1) rabbit polyclonal CGRP (1:1000, Millipore), (2) rabbit polyclonal SP (1:1000, Immunostar), (3) rabbit polyclonal IB4 (1:1000, Sigma Chemicals), (4) rabbit polyclonal mGluR5 (1:500, Epitomics) respectively at 4 ℃ overnight. After rinsing in Tris, the sections are incubated with biotinylated goat anti-rabbit IgG (1:100; Jackson ImmunoResearch Laboratories) for 1 h followed by avidin-biotin complex horseradish peroxidase reagent (Vector Laboratories) for another hour and the reaction products are demonstrated with 3,3'-diaminobenzidine (DAB, Sigma–Aldrich Co., St. Louis).

Imaging analysis

Areas with ir expression in the dorsal horn are quantified following a protocol modified from previously published methods (Swett and Woolf, 1985; Tseng et al., 2008). The principle of calculating ir expression in the laminae I and II of the dorsal horn is based on the marked differences in the optical densities between the ir expression and the background measured with Adobe Photoshop Elements 2.0 (San Jose). The numbers of ir expression on each side of the spinal cord and the areas of laminae I and II of the dorsal horn are measured as ir expression (μm^2) for each side of the spinal cord.

The principle of calculating IR expression in the laminae I and II of the dorsal horn was based on the marked differences in the optical densities between the IR expression and the background measured with Adobe Photoshop Elements 2.0 (San Jose). Except for measuring the optical densities of the defined IR expression and the background, no any processing of images such as changing the contrast or intensity was performed with this software. The optical density of the dorsal column was defined as the background optical density of that section, which was compared with the optical density of IR expression in the dorsal horn. The numbers of IR expression on each side of the spinal cord and the areas of laminae I and II of the dorsal horn were measured as IR expression (μm^2) for each side of the spinal cord. To eliminate variations among different rats and to reveal the difference between the operative and contralateral sides, a normalized ratio of IR area in expression (operative side/contralateral side) was derived as the dorsal horn index.

Double-labeled immunofluorescence

In brief, these foodpad skin sections are blocked with 5% normal goat serum with 0.5%

Triton X-100 in 0.5 M Tris for 1 h at room temperature and incubated with one of a mixture of primary antiserum at 4 ℃ overnight: (1) rabbit polyclonal mGluR5 (1:100, Epitomics)/mouse monoclonal CGRP (1:100, Santa Cruz), (2) rabbit polyclonal mGluR5 (1:100, Epitomics)/mouse monoclonal SP (1:100, Santa Cruz), and (3) rabbit polyclonal mGluR5 (1:100, Epitomics, Burlingame)/biotinated IB4 (1:100, Sigma Chemicals). After rinsing in Tris, sections are incubated with a mixture of secondary antibodies for another hour, i.e., (1) fluorescein FITC-conjugated anti-rabbit IgG and (2) Texas Red-conjugated anti-mouse IgG (both 1:100 and purchased from Jackson ImmunoResearch Laboratories). The sections are then dehydrated with 50% and 100% glycerol, mounted in VectoShield (Vector Laboratories), covered with a coverslip, and photographed under a conventional epifluorescent microscope (Zeiss Axiophot, Carl Zeiss) equipped with appropriate filters.

Statistical Analysis

Examiners were blinded to the grouping information when performing all the laboratory procedures of measurement and quantitation. Values are expressed as mean ± standard deviation using GraphPad Prism (GraphPad, San Diego, CA, USA). Statistical comparisons in behavioral assessments and dorsal horn area were made by a one-way repeated measures analysis of variance (ANOVA), followed by Bonferroni *post hoc* test, with the times as the within-subjects factor. Statistical comparisons in pharmacological intervention were made by the two-way ANOVA, followed by Bonferroni *post hoc* test, with the concentrations of a TLR5 agonist as between-subjects factors and time as the within-subjects factor. A probability value of less than 0.05 ($p < 0.05$) was considered statistically significant.

結果與討論（含結論與建議）

We performed nerve decompression in CCI model, to investigate a potential mechanism of mGluRs/PKC signaling for pain memory, which provided alternative therapeutic strategies for targeting medications.

Nerve Decompression Efficiently Relieved CCI-Induced Pain Hypersensitivity

To examine the influence of nerve decompression in relieving pain hypersensitivity after CCI, we conducted behavioral assessments and compared the difference between CCI and Decompression groups (Figure 1). In CCI group, the decreases of withdrawal threshold were revealed on ipsilateral sides, indicating mechanical hyperalgesia, from post-operative week (POW) 2 to POW 8 ($p < 0.0001$ v.s. Sham) (Fig. 1A). More importantly, in Decompression group, withdrawal thresholds showed on ipsilateral sides have no considerable difference with that on contralateral sides at POW 8 ($p = 0.6066$) (Figure 1A). Likewise, the reductions of mechanical threshold on ipsilateral sides were shown in CCI

group during the entire experimental period ($p < 0.0001$) (Fig. 1B). At POW 8 in Decompression group, mechanical thresholds on ipsilateral sides revealed similar outcomes as which measured on contralateral sides ($p = 0.4158$) (Figure 1B).

Nerve Decompression Modulated the Reversal of Synaptic Plasticity in Dorsal Horn

To recognize the influence of nerve decompression in CCI-induced changes of synaptic plasticity in dorsal horn, we applied immunohistochemical staining with antiserums against CGRP, SP and IB4 (Fig. 2, 3, and 4). On contralateral sides, peptidergic C and Aδ terminals were illustrated by CGRP-ir expression, which showed dense varicosities in lamina I, the outer part of lamina II and even lamina V (Fig. 2 C). However, on the ipsilateral sides, there was not a noticeable difference in CGRP-ir expression at POW 8 between CCI and Decompression groups (Fig. 2 A, B). Similarly, SP is known as a marker of unmyelinated C terminals. On contralateral sides, SP-ir expression showed beaded particles mostly in lamina I and extended to the outer part of lamina II (Fig. 3 C). At POW 8, partial loss of SP-ir expression in the equivalent laminae was detected on ipsilateral sides in CCI group (Fig. 3 A). Also, on the ipsilateral sides, Decompression group showed more abundant SP-ir expression in the corresponding laminae (Fig. 3B). Besides, IB4 is also known as a marker of unmyelinated C terminals. IB4-ir expression on contralateral sides which exhibited irregular structures expressed generally in the inner part of lamina II (Fig. 4 C). On ipsilateral sides, a reduction of the amount of IB4-ir expression was observed at POW 8 in CCI group (Fig. 4 A). In contrast, an observable increase of IB4-ir expression was revealed on the ipsilateral sides in Decompression group (Fig. 4B).

We verified the temporal changes of CGRP-, SP-, and IB4-ir expression by quantitation of ir dorsal horn index in dorsal horn (Fig. 2, 3, and 4). As the results demonstrated, CGRP-ir dorsal horn index in Decompression group were similar to those in CCI group ($p = 0.9513$) (Fig. 2 D). At the same time point, SP-ir dorsal horn index revealed a significant increase in Decompression group at POW 8 (vs. CCI group, $p < 0.05$) (Fig. 3 D). Importantly, a noticeable increase of IB4-ir dorsal horn area was also detected in Decompression group at POW 8 (vs. CCI group, $p < 0.05$) (Figure 4 D).

CCI-induced decrease of mGluR5-ir expression in dorsal horn was reversed by nerve decompression

To recognize whether the synaptic plasticity of mGluR5 changed as a result of nerve decompression in CCI rats, we studied the mGluR5-ir expression in dorsal horn through immunohistochemistry (Fig. 5). In Sham, slight mGluR5-ir expression exhibited a dense dot-like appearance mainly in the inner part of lamina II (Fig. 5 C). Comparatively, images revealed a more obvious increase of mGluR5-ir expression in CCI group than that in

Decompression group at POW 8 (Figure 5 A, B). We verified the temporal changes of mGluR5-ir expression by quantitation of mGluR5-ir dorsal horn index (Fig. 5 D). In CCI group, values exhibited a large increase of mGluR5-ir dorsal horn index through the end of experiments ($p < 0.01$). More importantly, at POW 8 in Decompression group, values of mGluR5-ir dorsal horn index decreased to the level of close to those in Sham ($p = 0.0929$).

Increase of mGluR5 expression was predominantly associated with IB4 Expression after Nerve Decompression

In order to determine the actual mGluR5-ir expression in dorsal horn, double immunofluorescence was applied to evaluate its co-expressions with peptidergic or non-peptidergic terminals (Fig. 6). At POW 8, mGluR5- and CGRP-ir expressions in both groups co-expressed around the border between the outer and inner part of lamina II (Fig. 6 A, B). Moreover, it showed that mGluR5- and SP-ir expressions were not meaningfully co-expressed in both groups in lamina I (Fig. 6 C, D). It is surprising that mGluR5-ir expression almost co-expressed with IB4-ir expression mainly in the inner part of lamina II in CCI group (Fig. 6 E). This phenomenon of co-expression between TLR5- and IB4-ir expressions was also detected significantly in Decompression group (Fig. 6 F). In summary, these above findings confirmed the facts in Decompression group that decrease of mGluR5-ir expression was significantly associated with non-peptidergic terminals, which were unmyelinated C terminals, in dorsal horn.

結論與建議

Here, we propose the nerve decompression attenuates CCI-induced mechanical hypersensitivity through the modulation of mGluRs/PKC signaling, sequential hypothesis including: (1) nerve decompression changes the plasticity of peptidergic (calcitonin gene-related peptide (CGRP) and substance P (SP)) and non-peptidergic (Isolectin B4 (IB4)) nerve terminals in the spinal cord; (2) spinal plasticity of mGluRs, including subtype 1 and 5 (mGluR1 and mGluR5), are altered following nerve decompression; (3) in addition, classical protein kinase c (PKC) is the possible downstream modulator of mGluRs; (4) in CCI, the treatment of lentiviral vector expressing Hes1 by intra-DRG injections inhibits the synthesis of mGluRs in the spinal cord.

About the potential spinal mechanisms of mechanical hypersensitivity in rats with CCI, our preliminary results indicate that (1) nerve decompression attenuates mechanical allodynia and hyperalgesia significantly; (2) nerve decompression do not change the spinal plasticity of CGRP-immunoreactive (ir) nerve terminals; (3) in contrast, IB4-ir nerve terminals is increased in the lamina II of the spinal cord after nerve decompression; (4) nerve decompression results in the decrease of CCI-induced activation of mGluR5 in the lamina

II of the spinal cord.

Currently, much of our morphological evidence points to strong associations rather than specific mechanisms of action, which also implicate mGluR5-ir nerve terminals in the spinal cord as necessary for the induction of mechanical hypersensitivity. Therefore, treatment of lentiviral vector expressing Hes1 gene to inhibit the synthesis of mGluR5 via intra-DRG injections may be a potentially useful tool to screen for truly mGluR5-dependent mechanical hypersensitivity in rats with CCI whereas this therapy may be most effective and beneficial.

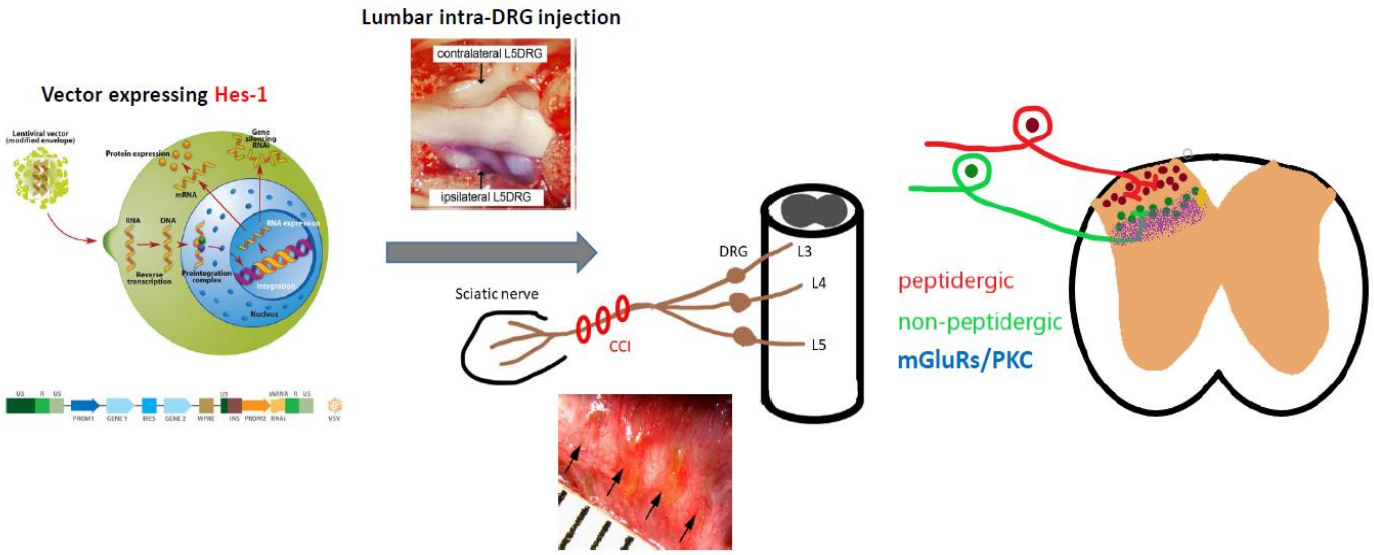

本實驗研究計畫之重要性：

周邊神經受到壓迫造成損傷則是建立神經病變引發疼痛行為反應的基礎，包括了慢性壓迫傷害(Chornic constrition injury (CCI))，部分坐骨神經緊綁傷害(Partial sciatic nerve ligation (PSNL))和脊髓神經緊綁傷害(Spinal nerve ligation (SNL))(Bennett and Xie, 1988; Kim and Chung, 1992; Seltzer et al., 1990)。手術性的解除神經壓迫方式(Surgical decompression)，通常在臨床上被用來減輕神經病變引發的疼痛反應症狀，例如：腕隧道症狀(Carpal tunnel syndrome)，脊神經根壓迫(Spinal root compression)和血管壓迫造成的三叉神經痛(Trigeminal neuralgia due to vascular compression)(Love and Coakham, 2001; Binder et al., 2002; Steinberg, 2002; Thoma et al., 2004)。理論上，幾個潛在的機制強調在手術性的解除壓迫後可以減緩或消除神經病變而引發的疼痛反應，這些機制包括：用以重建表皮神經與其標地物聯絡的表皮神經纖維再生(Epidermal nerve regeneration)；以及在中樞神經系統，脊髓背角中來自背根神經節內神經元的中樞神經軸突突觸的塑性改變和中樞脊髓背角中中間聯絡神經元內訊息傳遞路徑的活化與抑制(George et al., 2000; Suzuki and Dickenson, 2005; Woolf et al., 1998; Woolf, 2000; Woolf, 2004; Woolf and Salter, 2006)。

參考資料

1. Padua L, Coraci D, Erra C, Pazzaglia C, Paolasso I, Loreti C, Caliandro P, Hobson-Webb LD (2016) Carpal tunnel syndrome: clinical features, diagnosis, and management. Lancet Neurol 15:1273-1284.

2. Thomson JG (2017) Diagnosis and treatment of carpal tunnel syndrome. Lancet Neurol. 16:263.
3. Bennett GJ, Xie YK (1988) A peripheral mononeuropathy in rat that produces disorders of pain sensation like those seen in man. Pain 33:87-107.
4. Tseng TJ, Chen CC, Hsieh YL, Hsieh ST (2007a) Effects of decompression on neuropathic pain behaviors and skin reinnervation in chronic constriction injury. Exp Neurol 204:574-582.
5. Tseng TJ, Chen CC, Hsieh YL, Hsieh ST (2008) Influences of surgical decompression on the dorsal horn after chronic constriction injury: changes in peptidergic and delta-opioid receptor (+) nerve terminals. Neuroscience 156:758-768.
6. Todd AJ (2010) Neuronal circuitry for pain processing in the dorsal horn. Nat Rev Neurosci 11:823-836.
7. Ji RR, Kohno T, Moore KA, Woolf CJ (2003) Central sensitization and LTP: do pain and memory share similar mechanisms? Trends Neurosci 26:696-705.
8. Woolf CJ (2000) Pain. Neurobiol Dis 7:504-510.
9. Tseng TJ, Yang ML, Hsieh YL, Ko MH, Hsieh ST (2018) Nerve decompression improves spinal synaptic plasticity of opioid receptors for pain relief. Neurotox Res. 33(2):362-376.
10. Tseng TJ, Hsieh YL, Hsieh ST (2007b) Reversal of ERK activation in the dorsal horn after decompression in chronic constriction injury. Exp Neurol 206:17-23.
11. Tseng TJ, Hsieh YL, Ko MH, Hsieh ST (2014) Redistribution of voltage-gated sodium channels after nerve decompression contributes to relieve neuropathic pain in chronic constriction injury. Brain Res 1589:15-25.
12. Crupi R, Impellizzeri D, Cuzzocrea S (2019) Role of Metabotropic glutamate_ receptors in neurological disorders. Front Mol Neurosci 12:20.
13. Obara I, Goulding SP, Hu JH, Klugmann M, Worley PF, Szumlinski KK (2013) Nerve injury-induced changes in Homer/glutamate receptor signaling contribute to the development and maintenance of neuropathic pain. Pain. 154(10):1932-45.
14. Pereira V, Goudet C (2019) Emerging Trends in pain modulation by metabotropic glutamate receptors. Front Mol Neurosci 11:464.
15. Khan A, Khan S, Kim YS (2019) Insight into pain modulation: nociceptors sensitization and_therapeutic targets. Curr Drug Targets 20(7):775-788.
16. Price TJ, Inyang KE (2015) Commonalities between pain and memory mechanisms and their meaning for understanding chronic pain. Prog Mol Biol Transl Sci 131:409-34.
17. Wang JQ, Guo ML, Jin DZ, Xue B, Fibuch EE, Mao LM (2014) Roles of subunit phosphorylation in regulating glutamate receptor function. Eur J Pharmacol 728:183-7.
18. Mochly-Rosen D, Das K, Grimes KV (2012) Protein kinase C, an elusive therapeutic target? Nat Rev Drug Discov 11(12):937-57.
19. Zimmermann M (1983) Ethical guidelines for investigations of experimental pain in conscious animals. Pain 16:109-110.
20. Hsieh MC, Peng HY, Ho YC, Lai CY, Cheng JK, Chen GD, Lin TB (2019) Transcription Repressor Hes1 Contributes to Neuropathic Pain Development by Modifying CDK9/RNAPII-Dependent Spinal mGluR5 Transcription. Int J Mol Sci 20(17).
21. Chang MF, Hsieh JH, Chiang H, Kan HW, Huang CM, Chellis L, Lin BS, Miaw SC, Pan CL, Chao CC, Hsieh ST (2016) Effective gene expression in the rat dorsal root ganglia with a non-viral vector delivered via spinal nerve injection. Sci Rep 6:35612.

附圖

Fig. 1. Effects of nerve decompression on chronic constriction injury (CCI)-induced mechanical hypersensitivity. The temporal changes of hypersensitivity were shown in (A) mechanical hyperalgesia and (B) mechanical allodynia. The threshold of pinprick was demarcated as withdrawal threshold (g) and the threshold stimulated by Von Frey filaments was determined as mechanical threshold (g). Behavioral assessments were expressed as the mean ± SD (n = 3 in each group at each PIW). ***$p < 0.001$, indicated as a significant difference compared with Sham. ###$p < 0.001$, indicated as a significant difference between CCI and Decompression.

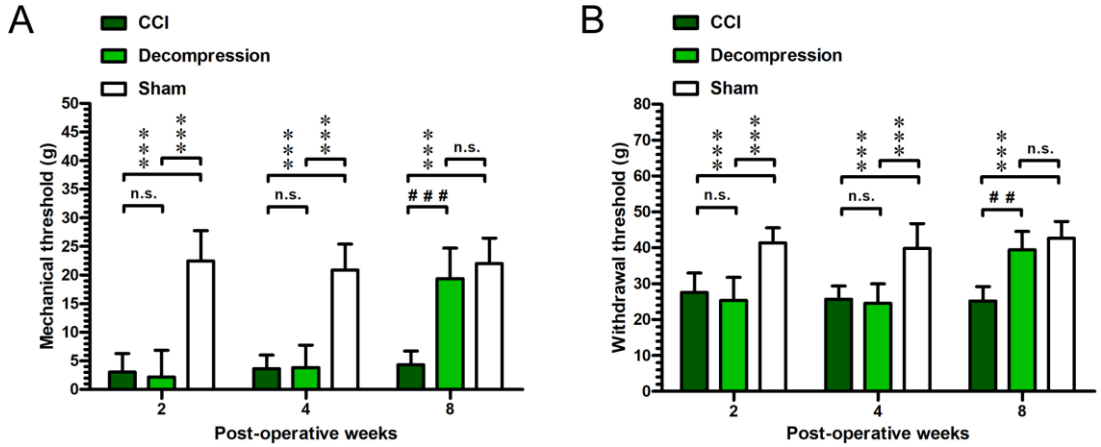

Fig. 2. Effects of nerve decompression on calcitonin gene-related peptide (CGRP)-immunoreactive (ir) expression in the spinal cord. At POW 8, reductions of CGRP-ir expression were still detected in the spinal cord in both (A) CCI and (B) Decompression. (C) Images show the standard pattern of CGRP-ir expression on the Sham, whereas these abundant dense varicosities were mainly expressed in the laminae I of the dorsal horn. Scale bars, 100 μm. (D) Histograms showed the data of dorsal horn index for CGRP-ir expressions in the spinal cord, i.e., the ratio of ir area in the dorsal horn (operative side/contralateral side). Temporal patterns of dorsal horn index were compared with Sham to illustrate the changes of CGRP-ir expression in the spinal cord. ** $p < 0.01$ and *** $p < 0.001$, indicates a significant difference at the same time point.

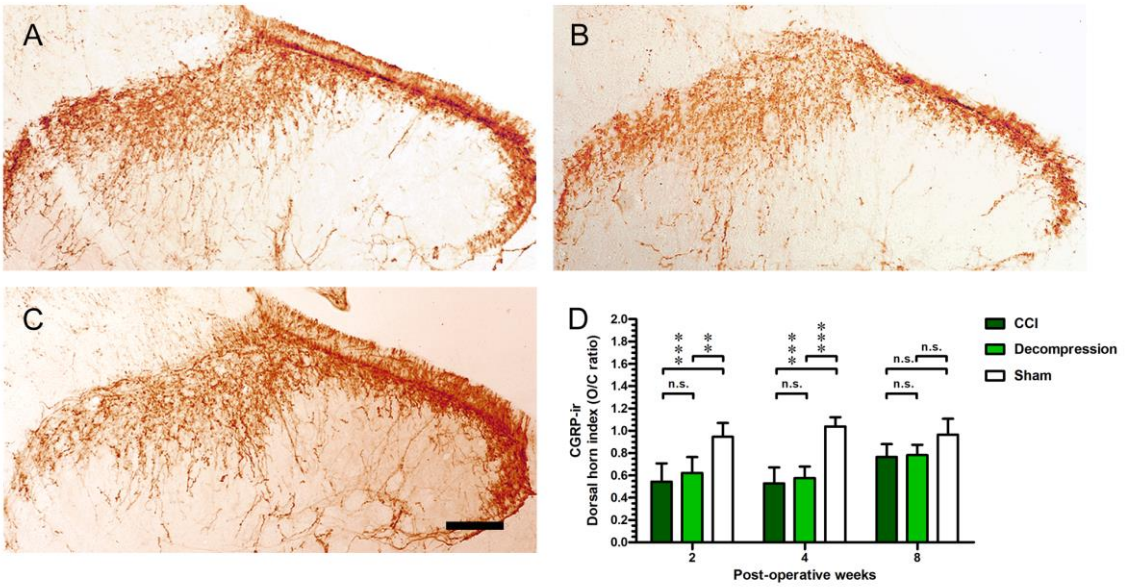

Fig. 3. Effects of nerve decompression on substance P (SP)-ir expression in the spinal cord. At POW 8, reductions of SP-ir expression were still detected in the spinal cord in both (A) CCI and (B) Decompression. (C) Images show the standard pattern of CGRP-ir expression on the Sham, whereas these abundant dense varicosities were mainly expressed in the laminae I of the dorsal horn. Scale bars, 100 μm. (D) Histograms showed the data of dorsal horn index for CGRP-ir expressions in the spinal cord, i.e., the ratio of ir area in the dorsal horn (operative side/contralateral side). Temporal patterns of dorsal horn index were compared with Sham to illustrate the changes of CGRP-ir expression in the spinal cord. ** $p < 0.01$ and *** $p < 0.001$, indicates a significant difference at the same time point. # $p < 0.05$, indicated as a significant difference between CCI and Decompression.

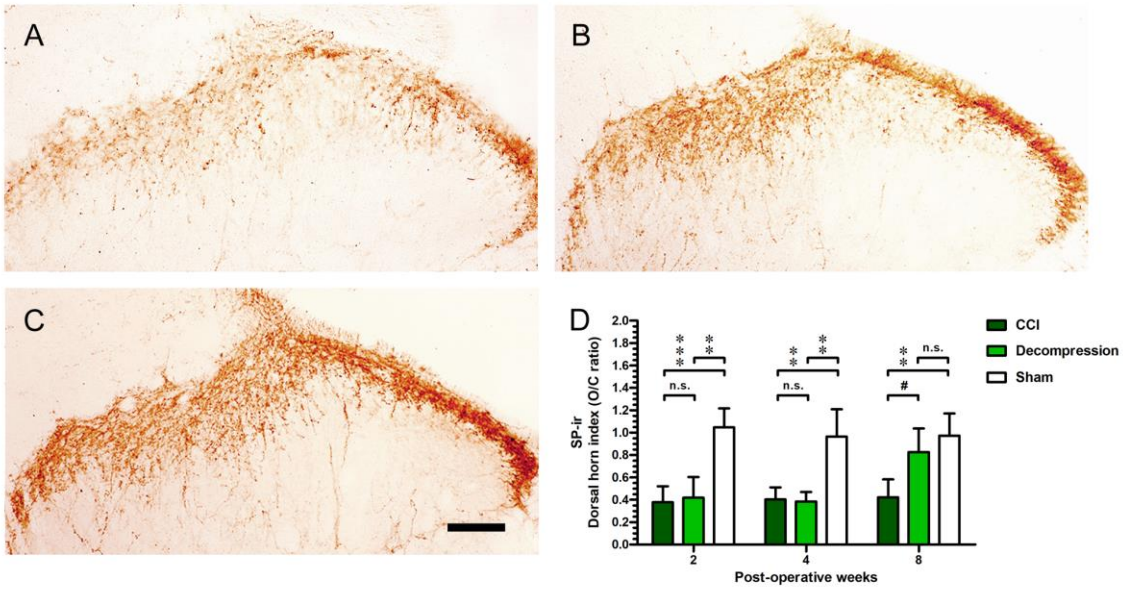

Fig. 4. Effects of nerve decompression on Isolectin B4 (IB4)-ir expression in the spinal cord. At POW 8, (B) reductions of IB4-ir expression were noticed in the spinal cord. (C) Prominently, in Decompression, IB4-ir expressions were increased. (C) Images show the standard pattern of IB4-ir expression on the Sham, whereas these abundant dense varicosities were mostly expressed in the laminae II of the dorsal horn. Scale bars, 100 μm. (D) Histograms showed the data of dorsal horn index for IB4-ir expressions in the spinal cord, i.e., the ratio of ir area in the dorsal horn (operative side/contralateral side). Temporal patterns of dorsal horn index were compared with Sham to illustrate the changes of IB4-ir expression in the spinal cord. ** $p < 0.01$ and *** $p < 0.001$, indicates a significant difference at the same time point. # $p < 0.05$, indicated as a significant difference between CCI and Decompression.

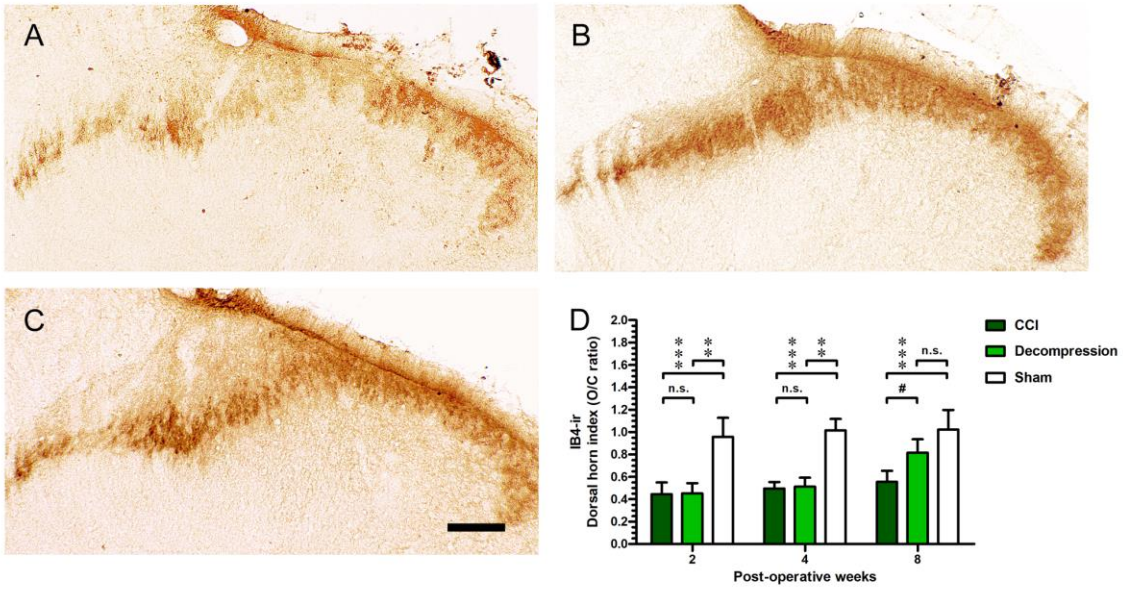

Fig. 5. Effects of nerve decompression on metabotropic glutamate receptor subtype 5 (mGluR5)-ir expression in the spinal cord. At POW 8, (A) images show the standard pattern of mGluR5-ir expression on the Sham, whereas these common dense varicosities were generally expressed in the laminae II of the dorsal horn. (B) Significant increases of mGluR5-ir expression were observed in the spinal cord. (C) Importantly, mGluR5-ir expressions were decreased in Decompression. Scale bars, 100 μm. (D) Histograms showed the data of dorsal horn index for mGluR5-ir expressions in the spinal cord, i.e., the ratio of ir area in the dorsal horn (operative side/contralateral side). Temporal patterns of dorsal horn index were compared with Sham to illustrate the changes of mGluR5-ir expression in the spinal cord. * $p < 0.05$ and ** $p < 0.01$, indicates a significant difference at the same time point. # $p < 0.05$, indicated as a significant difference between CCI and Decompression.

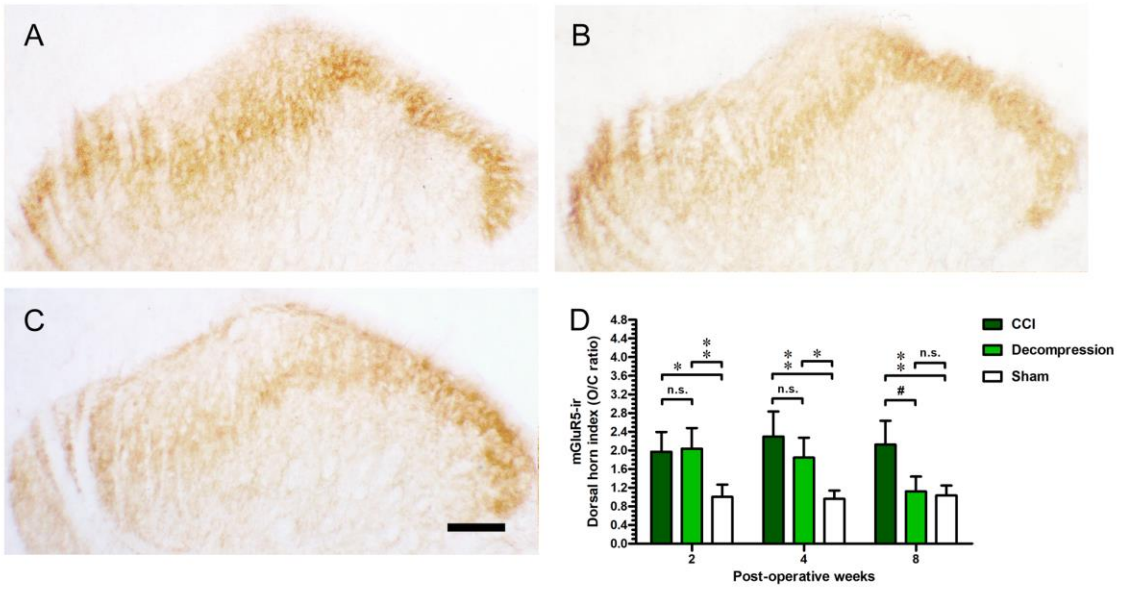

Fig. 6. Identification of mGluR5 expression in dorsal horn by double immunofluorescence. (A, C, E) CCI and (B, D, F) Decompression groups exhibited their related co-expressions in the medial portion of dorsal horn at POW 8. (A, B) The merged images illustrated the increase of mGluR5-ir (green) expression in CCI and Decompression group slightly co-expressed with CGRP-ir (red) expression in lamina I. (C, D) In the merged images,

TLR5- (green) and SP-ir (red) expressions partially co-expressed, especially near the border between the outer and inner part of lamina II. (E, F) Importantly, mGluR5-ir (green) expression mainly co-expressed with IB4-ir (red) expression in the inner part of lamina II. Also, the similar pattern of mGluR5- and IB4-ir co-expression was demonstrated in CCI group. Scale bar = 40 μm.

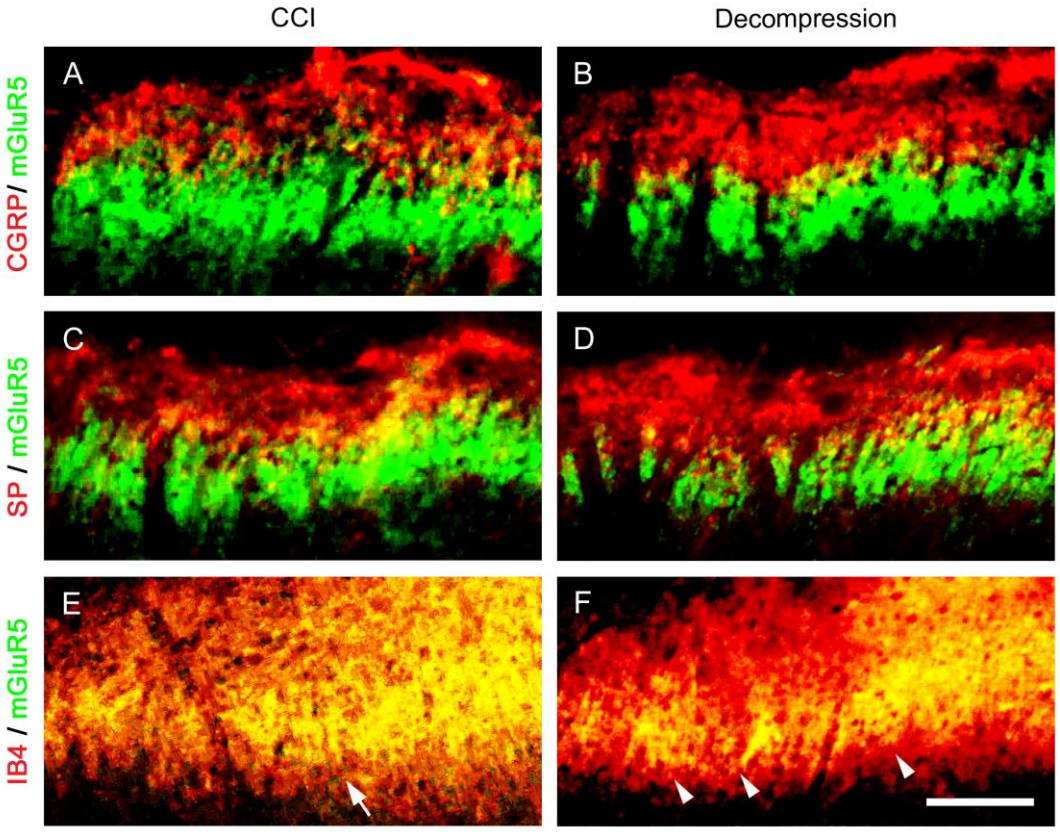

表 C802